



HAL
open science

Quasi-Dynamic Line Rating spatial and temporal analysis for network planning

Stella Hadiwidjaja, Sergio Daniel Montana Salas, Andrea Michiorri

► **To cite this version:**

Stella Hadiwidjaja, Sergio Daniel Montana Salas, Andrea Michiorri. Quasi-Dynamic Line Rating spatial and temporal analysis for network planning. 2023. hal-03766110v2

HAL Id: hal-03766110

<https://minesparis-psl.hal.science/hal-03766110v2>

Preprint submitted on 23 Jan 2023

HAL is a multi-disciplinary open access archive for the deposit and dissemination of scientific research documents, whether they are published or not. The documents may come from teaching and research institutions in France or abroad, or from public or private research centers.

L'archive ouverte pluridisciplinaire **HAL**, est destinée au dépôt et à la diffusion de documents scientifiques de niveau recherche, publiés ou non, émanant des établissements d'enseignement et de recherche français ou étrangers, des laboratoires publics ou privés.

QUASI-DYNAMIC LINE RATING SPATIAL AND TEMPORAL ANALYSIS FOR NETWORK PLANNING

Stella HADIWIDJAJA
NUS – Singapore

stella.hadiwidjaja@u.nus.edu

Sergio Daniel MONTANA SALAS
Mines Paris – PSL – France

sergio-daniel.montana-salas@minesparis.psl.eu

Andrea MICHIORRI
Mines Paris – PSL – France

andrea.michiorri@minesparis.psl.eu

1 **ABSTRACT**

2 *This study proposes a methodology to design a quasi-Dynamic Line Rating, based on historical ampacity simulations using*
3 *weather reanalysis. As opposed to the static rating, this implementation of qDLR varies the current-carrying limit every*
4 *hour of every month, allowing a higher percentage of an overhead line's capacity to be utilized whilst reducing operational*
5 *risk. The methodology proposed can be applied to an existing transmission or distribution overhead line to improve its*
6 *performance or to a geographical region to support network planning.*
7 *The application of the methodology on an example overhead line shows significant potential gains in transmission capacity,*
8 *notably due to ampacity increases in the absence of solar radiation. The example also demonstrates better accommodation*
9 *of low ampacity events during hot weather, potentially improving network operating safety. Its application on the regional*
10 *level reveals potential ampacity bottleneck locations.*

11 **INTRODUCTION**

12 Electricity transmission networks face growing energy demand from human activities. Furthermore, several technologies
13 such as variable renewable energy sources and electric vehicles, can significantly increase power flow peaks. On the other
14 hand, network reinforcements are often economically challenging, socially unwelcome and time-consuming [1]. The current
15 carried by an overhead transmission line is called 'Ampacity'. It is limited by design for safety reasons and to avoid annealing
16 to a maximum continuous operating temperature, in the range 75-90°C. This value is continuously varying in real time due
17 to changing cooling conditions around the cable. The standard practice is to set a single conservative limit for each season
18 ('Summer', 'Winter' and 'Spring\Autumn'), referred to as a 'static' or 'seasonal' line rating. As this rating is designed to be
19 below the line's smallest ampacity throughout the season, networks are often performing substantially below their maximum
20 or average capacity [2]. In Section 2, the paper describes the methodology to develop an alternative qDLR, varying by the
21 hour and by month according to ampacity simulations based on historical weather data and conductor specifications. The
22 methodology can be applied to an existing line to improve its performance or a region to aid in optimizing network
23 reinforcements. The rating is 'quasi-Dynamic' as it compromises between the static line rating and the dynamic line rating,
24 which uses continuous monitoring to dynamically adjust the rating. The advantage is that qDLR are static and known in
25 advance by network operators and don't requires dynamic monitoring and control. The disadvantage is that their performance
26 is still below the average of the real component ampacity.

27 After a description of the background, the qDLR methodology is applied to an example transmission line and region. The
28 potential improvements observed, and its applications are discussed.

29 **BACKGROUND**

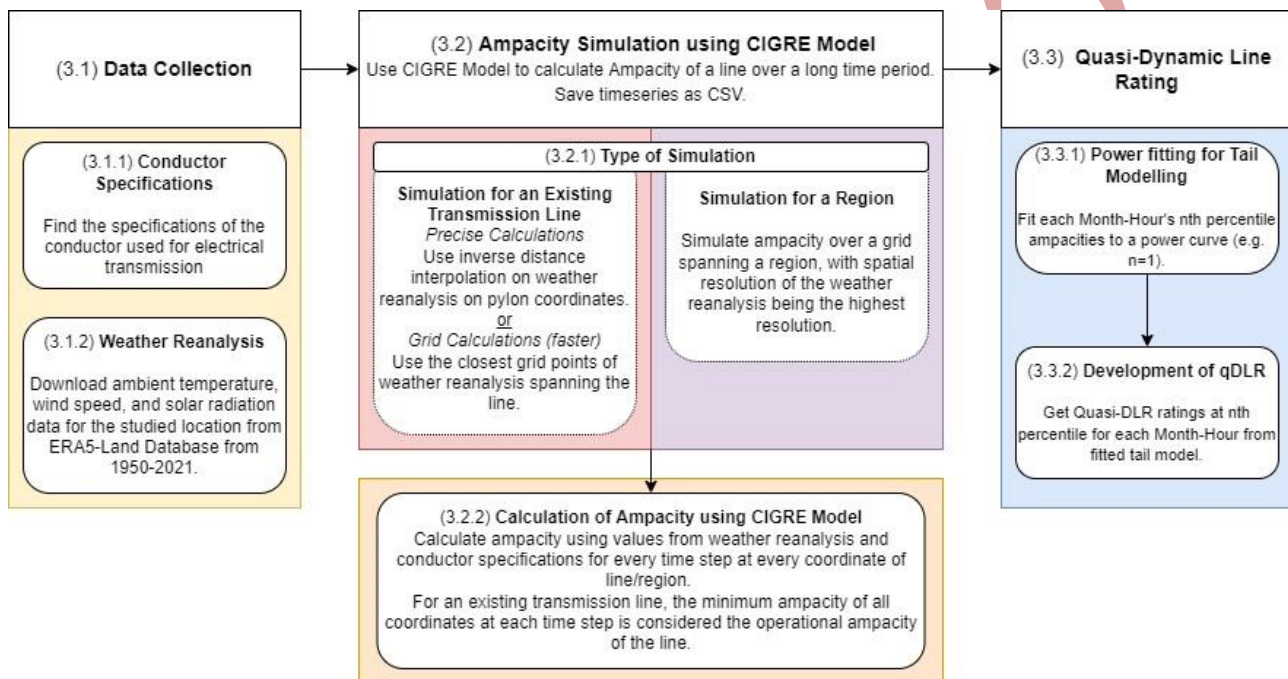
30 As current flows in an electric cable, the Joule effect causes it to heat up. Heating poses a safety concern as it leads to
31 excessive sagging of the conductor, increasing the transmission line's probability of collision with trees and infrastructure,
32 as well as short-circuit. Excessive temperatures can also lead to conductor annealing, reducing permanently tensile strength
33 and conductivity. Thus, an overhead line is limited by its ampacity, the maximum current an electric cable can carry whilst
34 meeting design and safety criteria to avoid excessive heating.

35 Ampacity can therefore be considered a measure of a conductor's ability to dissipate Joule heat. In turn, heat dissipation
36 depends on the weather: high temperatures, low wind speeds, and intense solar radiation impede heat dissipation, whilst low
37 temperature and high wind speeds accelerate it. Thus, ampacity decreases significantly on hot summer days, compared to
38 cold winter nights. Likewise, ampacity fluctuates according to cyclical meteorological changes (i.e. day/night, seasons). As
39 the weather varies geographically as well, the ampacity of a line is limited by few thermal bottlenecks on its length.

40 In alternative to the standard approach of applying static seasonal rating, it is often proposed the application of Dynamic
41 Line Rating [3]. In this approach, the ampacity is calculated in real-time thanks to measurements on or around the conductor.
42 This approach allows to extract the maximum allowable power transmission for each line, removing thermal constraints on
43 most occasions. But it has several drawbacks which hindered its application up to now: i) the necessity to forecast DLR to
44 account for them in operational planning and ii) the need to deploy additional monitoring, communication and control
45 devices interfering with network protection. Regarding DLR forecasts, reviews are available in [2], [4] and the problem of

1 predicting high-reliability day-ahead DLR predictions is faced in [5]. Regarding the interaction between DLR and protection
 2 equipment, more information can be found in [6]. The approach proposed in this paper aims at dealing with these two issues:
 3 by calculating a static rating for each hour-month combination and a pre-set accepted exceedance probability. This is simply
 4 the static seasonal rating approach but applied on a far higher temporal frequency. The same could be repeated with
 5 combinations of 4, 6 or 12 hours or seasons instead of months, but here the most detailed approach is studied. The advantages
 6 of such an approach are: i) ratings are known in advance at the planning or operational stage, ii) they can be embedded in
 7 protection equipment without the need for telecommunications, iii) they allow for a higher average ampacity, with peaks in
 8 the night, iv) they increase the safety of operation thanks to a finer definition of the intervals when probabilities are
 9 calculated, v) the possibility to tailor qDLR to each line. Of course, this approach has also drawbacks, notably: i) lower daily
 10 ampacities and ii) lower ampacities compared to DLR.

11 METHODOLOGY



12 Fig. 1: Methodology to develop Quasi-DLR

14 As mentioned in Section 1, using the standard static rating, the electric cables are operating well below their capacity most
 15 of the time, which limits electricity transmission in the network. At the same time, the overloading risk is not eliminated,
 16 especially in hot sunny hours. The main aim of qDLR is to increase this capacity whilst maintaining or improving operational
 17 safety.

18 This section describes the methodology to develop the qDLR, illustrated in Figure 1. The method involves first collecting
 19 the necessary environmental and conductor data. Then, the historical time series of ampacity is simulated on a collection of
 20 coordinates forming a grid or a line. Finally, a power distribution is fit to the tail-ends of the ampacity probability distribution,
 21 and the qDLR can be calculated according to a set conditional value at risk.

22 Data Collection

23 **Conductor Specifications**

24 In the case of an aluminium conductor-steel-reinforced (ACSR) cable, several specifications are required to calculate its
 25 ampacity, namely:

- 26 • D [mm] overall diameter of the conductor
- 27 • A [mm²] nominal area
- 28 • R_{dc} [km⁻¹Ω] resistance per unit length
- 29 • d [mm] non-ferrous diameter of one wire
- 30 • α [K⁻¹] temperature coefficient of resistance
- 31 • α_s : solar absorptivity of the surface
- 32 • ϵ_p : solar emissivity of the surface

D , A , R_{dc} , and d can be found in conductor tables from the provider of the cable. Default values of 0.5 for α_s and ϵ_p can be used in the case of lack of information [7].

Weather Reanalysis:

There are three weather variables needed for the calculation of Joule heat: ambient temperature, wind speed, and solar radiation. For wind direction, due to its high variability, a worst-case scenario of wind parallel to the conductor is assumed, considering that on the length of the overhead line circuit, almost all the directions are observed. These data are provided by a *reanalysis* dataset, which provides a comprehensive and consistent picture of the weather [8]. The reanalysis used in this paper is ERA5-Land, a dataset showing the hourly evolution of land variables from 1950 to 2021, with a resolution of $0.1^\circ \times 0.1^\circ$ (~ 10 km). The descriptive statistics of the weather from 1950-2021 of the 14 grid points spanning the example transmission line used can be found in Table I.

TABLE I: Sample Weather Data from 1950-2021 from ERA5Land around the line

	min	mean	max	std
t2m [°C]	-22.78	10.52	35.53	7.64
S [W/m ²]	0	150.89	1220.81	213.08
w10 [m/s]	0.0013	1.70	10.73	0.93

B. Ampacity Simulation

Type of Simulation:

Two types of simulation can be performed: on a specific set of coordinates (wherein lies an aerial electric cable), or on a grid spanning a region. Their respective purposes are to aid in improving the capacity of an existing transmission line or to optimise the expansion of the electrical network when routing new connections.

Simulation for an Existing Transmission Line: A list of coordinates (denoting the pylons of a transmission line, for example) is provided, and the weather data on each coordinate is gathered using inverse-distance interpolation of the reanalysis dataset (*Precise Calculations*).

Simulation for a Region: The desired bounding box coordinates are provided, and the ampacity at each grid point of the weather reanalysis is calculated. In the case of ERA5Land, the ampacity is calculated at a resolution of $0.1^\circ \times 0.1^\circ$ (~ 10 km between each point).

Ampacity calculation

The ampacity of each coordinate is calculated based on the CIGRE model for every hour in the period 1950-2021, for a given maximum allowable conductor temperature, T_{av} [7]. The CIGRE Model assumes the steady-state thermal condition of the conductor, in line with the hourly time step of the simulation. The heat gains and losses considered not negligible by the CIGRE model are solar heating, joule heating, radiative cooling and convective cooling. The power associated with these heat transfers depends on the conductor's specifications and the weather variables mentioned in Eq (1). By equating the heat gains and losses of the cable Eq (2), it determines the maximum joule heating allowable. From this, the maximum allowable current is deduced Eq (3).

$$P_j + P_s = P_r + P_c \quad (1)$$

Where P_j = Joule Heating

P_s = Solar Heating

P_r = Radiative Cooling

P_c = Convective Cooling

The maximum allowable DC current, I_{dc} , can then be calculated by imposing Joule Heating to be equal to net cooling.

$$P_j = I_{dc}^2 R_{dc}(1 + \alpha(T_{av} - 20)) \quad (2)$$

$$I_{dc} = \sqrt{\frac{P_r + P_c - P_s}{R_{dc}(1 + \alpha(T_{av} - 20))}} \quad (3)$$

In the case of a simulation for a single line, the minimum ampacity of each hour is the line's 'bottleneck', and is considered the operational ampacity.

C. Quasi Dynamic Line Rating

Power Fitting for Tail-Modelling

The power law is used to model the tail-end behaviour for each month-hour. By fitting the historical ampacities, the coefficients a and b which will be used to model I_{ac} is determined (4).

$$I_{ac} = ax^b \quad (4)$$

Where $I_{ac} = \text{Ampacity (A)}$

$x = \text{Percentile}$

$a, b = \text{Power Model Coefficients}$

Development of qDLR

Percentiles are the values below which a certain percentage of the data in a data set is found. According to the desired safety, the n_{th} percentile of each month-hour is calculated, where n is close to 1. For example, designing a rating to be at the first percentile ($n=1$) implies a 1% chance of the transmission line's ampacity being below the rating. If $n \ll 1$, the power fit may not be feasible. If $n \gg 1$, the tail model is no longer applicable, and the power fit is not appropriate to model the data.

3. RESULTS

The methodology described previously in Section 2 is applied to design a qDLR at the 1st and 0.1st percentile to a 225kV line in the French Riviera. The coordinate locations of the pylons and the grid points of the weather reanalysis spanning the line can be seen in Figure 2. The study assumes that:

- The static rating is also set at the historical ampacity's n^{th} percentile. For simplicity, *Summer* consists of June, July and August, *Winter* consists of December, January and February, and the rest are *Spring/Autumn*.
- The overhead line uses a continuous 'Drake' type ACSR conductor (see Table II)
- The maximum allowable cable temperature is 75 °C.

TABLE II: Conductor Specifications of DRAKE

Name	Area [mm ²]	Strands (Al) [n°]	D (Al) [mm]
DRAKE	402.83	26	4.44
Strands (Steel) [n°]	D (steel) [mm]	Overall D [mm]	Rdc [Ω/km]
7	3.45	28.11	0.07197

A. Minimum Ampacity

With the assumptions mentioned above, the ampacity of every span is calculated hourly in 1950-2021. A bottleneck can be observed in red around the minimum denoted by a star in Figure 2. The operating capacity is limited by the minimum ampacity through its length. Figure 3 thus demonstrates that the difference in weather patterns from location to location, even at a local level, can create a significant difference in transmission capacity, with differences up to 8% along several km and in the same hour.

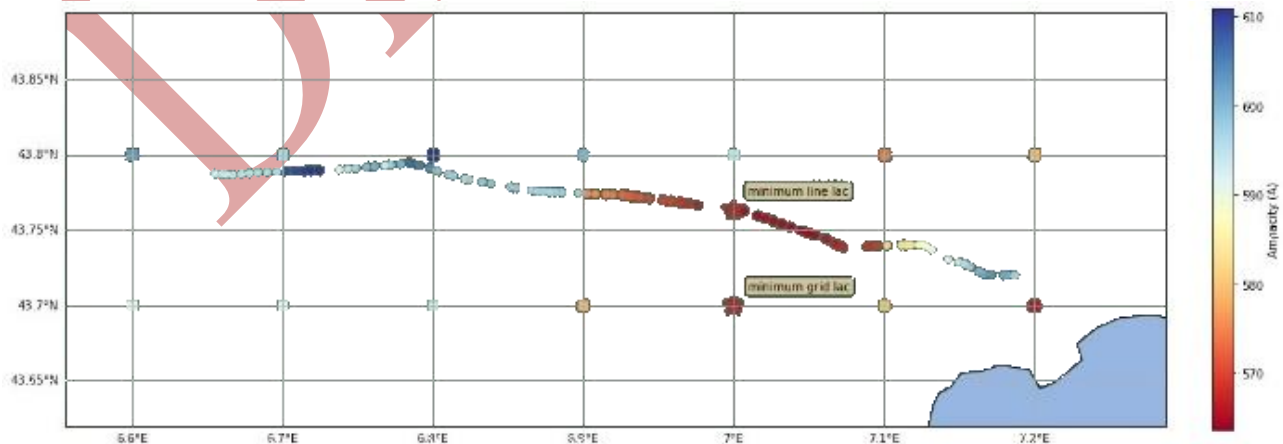


Fig. 2: Minimum ampacities for the studied overhead line

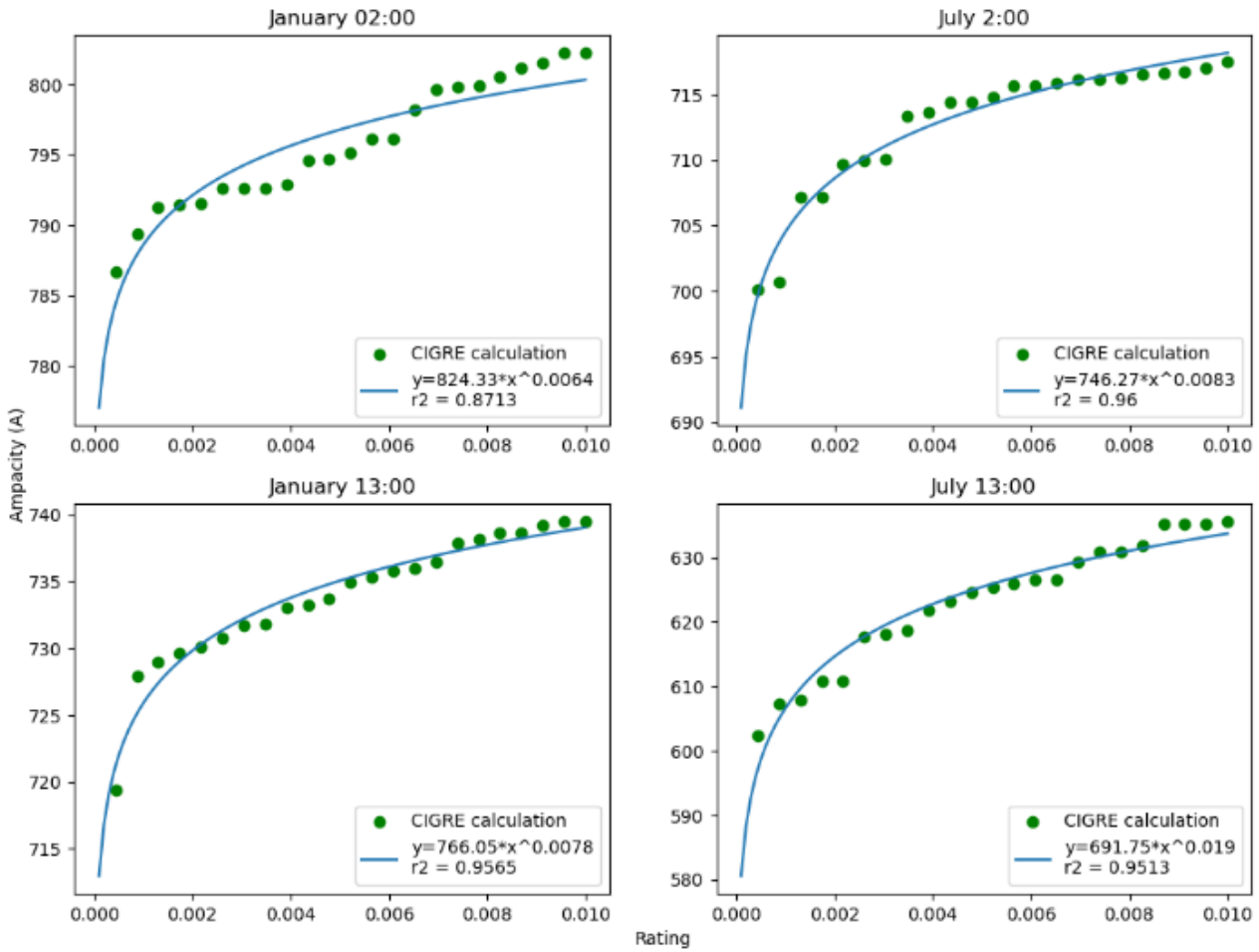


Fig. 3: Tail modelling for qDLR

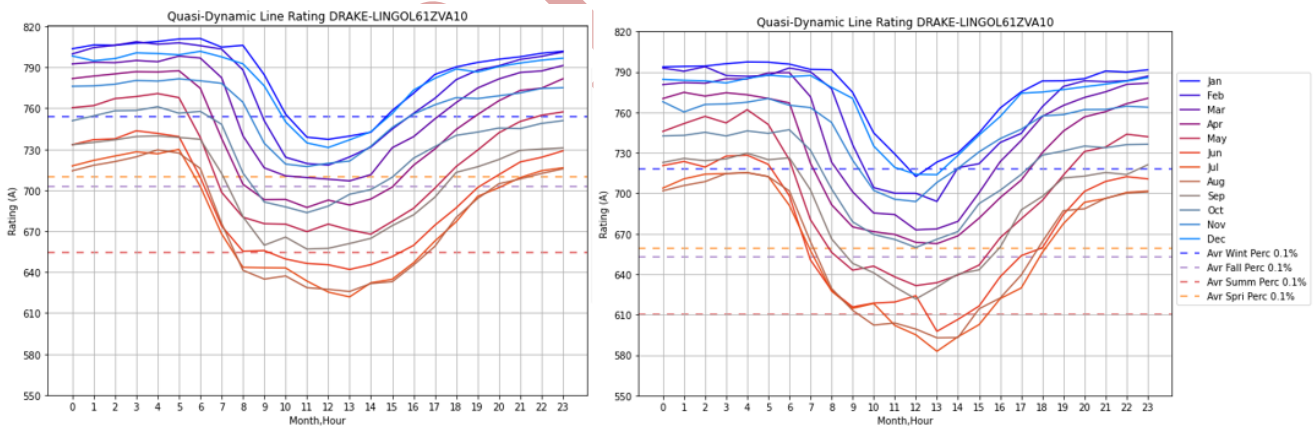
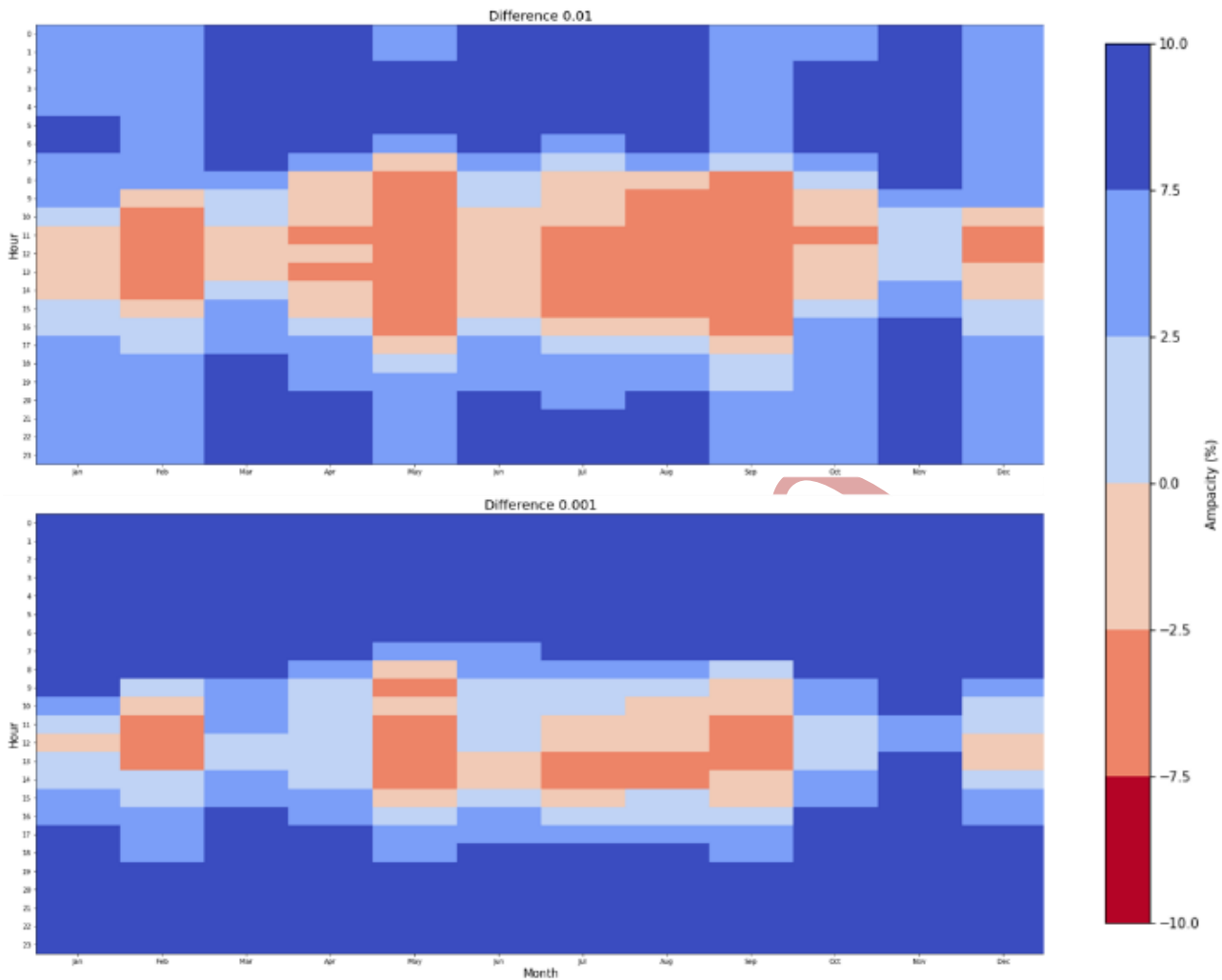


Fig. 4: qDLR for the studied line calculated with an exceedance probability of 1% (left) and 0.1% (right) and compared with the respective static seasonal ratings

1
2
3

4
5
6



1

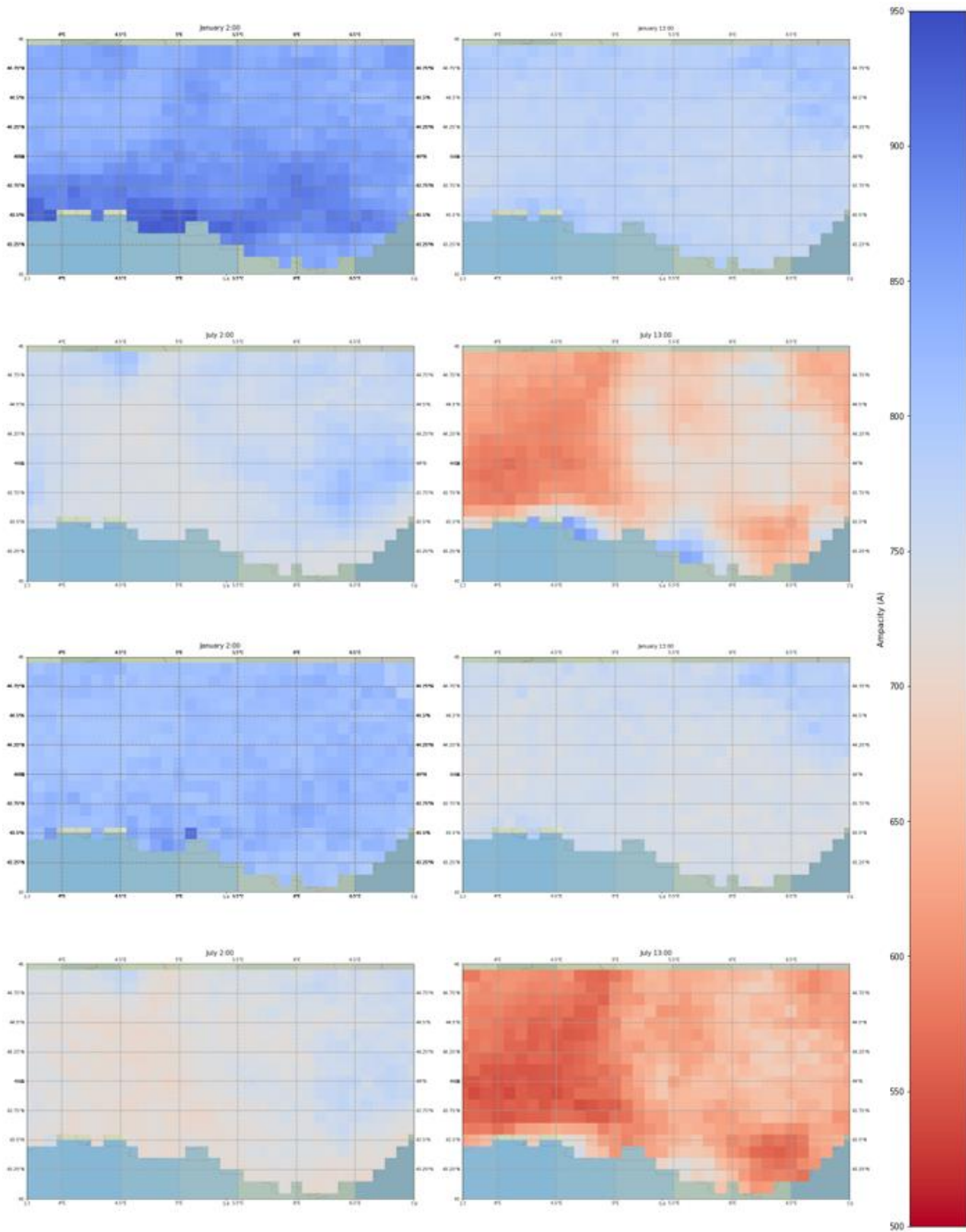
2 Fig. 5: Relative difference between qDLR and the respective static seasonal rating with an exceedance probability of 1%
 3 (above) and 0.1% (below)

4 The power law is used to model the lowest part of the distribution in the region below the 1st percentile for each month-hour
 5 combination. The average r is 0.94, demonstrating an apt fitting. Examples of the fitting in night and day of winter and
 6 summer are shown in Figure 3.

7 For $n > 1$, the data approaches a linear trend. On the other hand, for $n < 1$, there may be a lack of historical weather data to
 8 simulate enough ampacities for appropriate modelling as there are around 2130 instances of each month-hour in the 70 years
 9 used. This allows for only 21 data points at the 1st percentile.

10 **C. quasi-Dynamic Line Rating**

11 Using the tail models developed in Section 3-B, the qDLR can be calculated for any accepted overload probability for each
 12 month-hour period. These ratings compared to the equivalent static rating at the 1st percentile is shown in Figure 4 and the
 13 percentage difference in ampacity is shown in Figure 5. There is an overall average gain in the current capacity of 3.8%, a
 14 maximum increase of 14% (June 06:00), and a maximum decrease of -6.6% (September 11:00). Two notable differences are
 15 the ampacity gains during night-time and losses during the early afternoon. On the other hand, it must be noted that the
 16 ampacity reduction in daily hours corresponds also to an increase in safety.



1

2 Fig. 6: Examples of qDLR spatial variation in the PACA region calculated with an exceedance probability of 1% (above)
 3 and 0.1% (below). In both cases, it is represented a winter night (top left), a winter day (top right) a summer night (bottom
 4 left) and a summer day (bottom right)

Day and Night:

There are significant transmission capacity increases during night-time because of the lack of solar radiation. Especially during spring and summer, the ampacity can increase by almost 15% during the night, as seen in the blue areas in Figure 5. A steep descent and ascent in ampacity can be observed during sunrise and sunset respectively in Figure 4, demonstrating the influence of solar radiation on ampacity.

Early-Afternoon Heat:

qDLR consistently falls below the static rating during hot early afternoons, as seen in the orange regions of Figure 5. Using a qDLR can thus allow for more careful consideration of short daily periods of extreme heat, ensuring higher security of the network. Instances of abnormally low ampacities could become more relevant in some regions due to the climate context.

D. Grid Simulations

TABLE III: Spatial gradients in Ampacity (A/km)

mean	min	25%	50%	75%	max	std
0.62	-6.21	-0.47	-0.01	0.45	4.28	0.85

The methodology also allows for simulations over a region, in the form of a grid. As discussed in Section 3-A, and demonstrated by Figure 2, ampacity varies geographically. An example qDLR is done over the French PACA region, seen in Figure 6.

Descriptive statistics of the change in ampacity from one grid coordinate to its 8 nearest neighbours (in cardinal and ordinal directions) are shown in Table III. In general, the change in capacity (A/km) is not excessively dramatic, with an average and standard deviation of 0.62 and 0.85 respectively.

However, points with dramatic gradients can pinpoint bottlenecks, such as where the minimum gradient occurs, and where the change in ampacity reaches 6.21 A/km. Such information could potentially optimise the design of future overhead lines.

4. CONCLUSION

Transmission and distribution networks need higher capacities to keep pace with the rapid evolution of electricity production and consumption. This paper proposes a methodology to develop a qDLR for individual lines, varying the current-carrying limit for every month-hour combination based on ampacity simulations using historical weather reanalysis. The methodology can be applied to a set of coordinates representing an existing line, or a grid spanning a geographical area.

The study tested the methodology on an example transmission line in the South of France. The rating proposed showed an increase in transmission capacity over the equivalent 'static' rating of nearly 4%, whilst also increasing its security by safeguarding against low-ampacity events during hot weather. On the line considered, qDLR showed a maximum of 14% increase of the rating during periods of absence of solar radiation. During the early afternoon, the qDLR generally decreases, with a minimum of -7% capacity, safeguarding the line from extreme heat. In conclusion, the example demonstrates that qDLR can be used to improve the capacity of existing overhead lines.

The methodology was also applied to a sample region, the French Provence-Alpes-Cote d'Azur. The results show qDLR's ability to reveal geographical current capacity bottlenecks, which could be utilised in the design or reinforcement of transmission and distribution networks.

In conclusion, this paper proposes a methodology to develop a qDLR which could potentially improve current and future overhead lines by increasing their capacity and security without the need for expensive network expansions or reinforcements.

REFERENCES

- [1] Bruckner T., et al., Energy Systems. In: Climate Change 2014: Mitigation of Climate Change. Contribution of Working Group III to the Fifth Assessment Report of the Intergovernmental Panel on Climate Change, Cambridge University Press, Cambridge, United Kingdom and New York, NY, USA.
- [2] A. Michiorri et al., Forecasting for dynamic line rating, Renewable and Sustainable Energy Reviews, vol. 52, p. 1713-1730, dec. 2015, doi: 10.1016/j.rser.2015.07.134.
- [3] D. A. Douglass, Weather-dependent versus static thermal line ratings (power overhead lines), IEEE Transactions on Power Delivery, vol. 3, n 2, p. 742-753, avr. 1988, DOI: 10.1109/61.4313.
- [4] D. A. Douglass et al., A Review of Dynamic Thermal Line Rating Methods With Forecasting, IEEE Transactions on Power Delivery, vol. 34, n 6, p. 2100-2109, dec. 2019, doi: 10.1109/TPWRD.2019.2932054.
- [5] R. Dupin, L. Cavalcante, R. J. Bessa, G. Kariniotakis, et A. Michiorri, Extreme Quantiles Dynamic Line Rating Forecasts and Application on Network Operation, Energies, vol. 13, n 12, Art. n 12, janv. 2020, doi: 10.3390/en13123090.

- 1 [6] H. T. Yip et al., Dynamic thermal rating and active control for improved distribution network utilisation, p. 22-22, janv.
2 2010, doi: 10.1049/cp.2010.0213.
- 3 [7] Cigre WG 22.12, Thermal behaviour of overhead conductors , Electra, vol. 144, n 3, 1992
- 4 [8] Munoz Sabater, J., (2021): ERA5-Land hourly data from 1950 to 1980. Copernicus Climate Change Service (C3S)
5 Climate Data Store (CDS). (Accessed on 23-Feb-2020), 10.24381/cds.e2161bac
- 6 [9] Lignes aeriennes´, RTE – nouveau decoupage´ (au 2 decembre´ 2022)
- 7 <https://odre.opendatasoft.com/explore/dataset/lignes-aeriennesrte-nv/map/> (consulte le 16 janvier 2023).´

Draft V0.2